Chain Dynamics in Poly(*n*-alkyl acrylates) by Solid-State NMR, Dielectric, and Mechanical Spectroscopies

Marianne Gaborieau,*,† Robert Graf, Stefan Kahle, Tadeusz Pakula,‡ and Hans W. Spiess*

Max Planck Institute for Polymer Research, Ackermannweg 10, 55128 Mainz, Germany

Received March 19, 2007; Revised Manuscript Received June 11, 2007

ABSTRACT: A relaxation process was detected and quantified for the first time in various poly(*n*-alkyl acrylates) in the melt by a solid-state NMR method, NOE with dipolar filter. By comparison with dielectric spectroscopy and dynamic mechanical measurements carried out on the same samples, the relaxation process detected by NMR occurs at a higher temperature than the simple α-relaxation and on a longer time scale than the αβ-relaxation (cooperative α-relaxation). This relaxation process could be the isotropization of the main chain (by analogy with structurally similar polymethacrylates), but it is more probably a local relaxation within the alkyl side chain that is usually detected only at significantly lower temperatures. The fact that this side-chain motion is slower than the cooperative main-chain α-relaxation of restricted amplitude can be rationalized in the context of restricted amplitude main-chain motions in the local nanostructure present in the samples, as NMR and dielectric spectroscopy detect motions in different frames.

Introduction

Poly(alkyl acrylates) are of industrial importance due to their wide use in, e.g., pressure-sensitive adhesives (PSAs), paints, and coatings.[1] Most of those products are currently developed by trial-and-error procedures,[2] necessitating synthesis and tests of functional properties for numerous samples. Therefore, it is important to be able to characterize and understand the polyacrylate properties on a molecular level. On a long term, relating these to macroscopic properties (mechanical, adhesive) will allow one to directly design samples for specific applications rather than testing numerous samples.

In the present work, chain dynamics occurring in polyacrylate melts were investigated to gain insight into relaxation processes occurring on the molecular level. Poly(*n*-alkyl acrylate) homopolymers with various alkyl side chains were chosen as model samples for multicomponent poly(alkyl acrylate)-based industrial samples. We have recently developed a solid-state NMR method to quantify relaxation processes in homopolymers in the melt.[3] This method is based on measurements of relative motions of neighboring ^{1}H nuclei; thus, it is able to detect relaxation processes different from that usually detected by dielectric spectroscopy or dynamic mechanical measurements. It is applied to poly(*n*-alkyl acrylate) homopolymer melts in the present work. The results are compared with dielectric and dynamic mechanical results.

In poly(*n*-alkyl acrylates), short- and long-chain branching[4−6] as well as a local nanostructure[7,8] are present. The relaxation processes in polymers are influenced by long-chain branching, as shown for rheological properties of polyethylene.[9,10] Therefore, dielectric spectroscopy and dynamic mechanical analysis data used for comparison with results from the solid-state NMR method were measured on the *same samples*, rather than only taken from the literature. Furthermore, in order to characterize the local nanostructure, X-ray measurements were carried on the same samples.

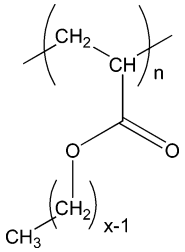

Figure 1. Chemical structure of poly(*n*-alkyl acrylate) samples: $x = 1$ for PMA, $x = 2$ for PEA, $x = 4$ for PBA, and $x = 6$ for PHxA.

The general formula of poly(*n*-alkyl acrylates) is shown in Figure 1. The homopolymers with the following alkyl side chains were synthesized: methyl (PMA, $x = 1$), ethyl (PEA, $x = 2$), butyl (PBA, $x = 4$), hexyl (PHxA, $x = 6$). Free-radical polymerization in solution was chosen to obtain broad molar mass distributions and branching levels similar to industrial samples and avoid the presence of surfactants.

Experimental Section

Materials.[11] Each *n*-alkyl acrylate (Aldrich, 98 or 99%, stabilized with hydroquinone or monomethyl ether hydroquinone) was distilled under pressure and stored at −20 °C. It was polymerized as a 4.7 mol L^{-1} solution in toluene initiated by 0.5 mol % of AIBN (azobis(isobutyronitrile)) with respect to the acrylic monomer. The polymerization was carried out at 60 °C under nitrogen for 20 h. The resulting reaction mixture was dissolved in an equal volume of dichloromethane. Then the polymer was precipitated in methanol at a temperature lower than its glass transition temperature (T_g), filtered, and finally dried in an oven (60 °C) under vacuum for one night. Please note that alkyl acrylates monomers are toxic and irritant and can induce sensitization.

The results of the characterization of the poly(*n*-alkyl acrylates) are given in Table 1. The T_gs were determined using differential scanning calorimetry (DSC) at 10 K min^{-1}; the detected T_g is in accordance with the values found in the literature[1] for each sample (taking into account the influence of the heating rate on the detected

* Corresponding authors. M.G.: Tel +61 7 3365 1865, Fax +61 7 3365 1188, e-mail m.gaborieau@uq.edu.au. H.W.S.: Tel +49 6131 379 120, Fax +49 6131 379 320, e-mail spiess@mpip-mainz.mpg.de.

† Current address: Centre for Nutrition and Food Sciences, Hartley Teakle building 83, The University of Queensland, Brisbane QLD 4072, Australia.

‡ Died on June 7, 2005.

10.1021/ma0706531 CCC: $37.00
Published on Web 07/24/2007

Table 1. Characterization of the Different Poly(*n*-alkyl acrylate) Samples

	PMA	PEA	PBA	PHxA
T_g (K)	294	259	227	213
M_n (g mol^{-1})	43000	163000	100000	88500
M_w (g mol^{-1})	229900	341000	318000	395000
M_w/M_n	5.3	2.1	3,2	4.5

T_g). ^{13}C NMR spectra in solution in $CDCl_3$ were recorded on a Bruker DRX500 at 125.76 MHz, with a relaxation delay of 10 s and 19 000−21 000 transients.[11] All samples are atactic, and their branching levels are several percent of the monomeric units. The average molar masses were determined via size exclusion chromatography (SEC) in THF with universal calibration using an online refractometer and viscometer; the experimental setup has been described elsewhere.[11] Since the polyacrylates are branched, their separation by SEC is not complete; thus, the newly developed formalism for proper determination of average molar masses of branched samples using hydrodynamic volumes distributions[12] has been used. More details on sample characterization are given in the Supporting Information.

Methods. *Dielectric Spectroscopy.* A broad-band dielectric spectrometer Novocontrol BDS 4000 (based on the high-resolution ALPHA analyzer) was used to measure the dielectric function $\epsilon^*(\omega) = \epsilon'(\omega) - i\epsilon''(\omega)$ at 10 points per frequency decade in a frequency range of $\omega/2\pi = 10^{-2}-10^{7}$ Hz and a temperature range from −120 to 100 °C. The sample capacitor consisted of two parallel gild brass plates with a diameter of 20 mm, separated by the sample. The plate distance of 0.1 mm was kept constant by small Teflon spacers.

According to linear response theory, the dielectric data can be also described by the corresponding complex dielectric modulus $M^*(\omega)$ where $\epsilon^*(\omega)M^*(\omega) = 1$ with $M^*(\omega) = M'(\omega) + iM''(\omega)$. Figure 2 shows the temperature and frequency dependence of the imaginary part of the dielectric modulus of the four polyacrylate samples. For each sample at least three relaxation processes were observed: conductivity contributions and segmental and local relaxations.

Using the nonlinear least-squares Levenberg−Marquardt method, each relaxation peak (M'') was fitted by the imaginary part M'' of the Havriliak−Negami (HN) funtion M^*:[13]

$$M^*(\omega) = M_\infty + \frac{\Delta M}{(1 + (i\omega\tau)^\alpha)^\gamma} \tag{1}$$

and

$$M''(\omega) = \Delta M \rho^{-\gamma} \sin(\gamma\theta) \tag{2}$$

with

$$\rho = \sqrt{(1 + 2\,(\omega\tau)^\alpha \cos(\pi\,\alpha/2) + (\theta\tau)^{2\alpha}} \tag{3}$$

and

$$\theta = A \tan\left[\frac{\sin(\pi\alpha/2)}{(\omega\tau)^{-\alpha} + \cos(\pi\alpha/2)}\right] \tag{4}$$

where $\omega = 2\pi\nu$ is the angular frequency and ΔM the intensity of the process. The maximum loss frequency ω_{max} for each process was analytically calculated from the fit parameters by[14]

$$\omega_{max} = \frac{1}{\tau}\left(\frac{\sin[\pi\alpha/2]}{\tan[\pi\alpha/2(\gamma+1)]} - \cos[\pi\alpha/2]\right)^{-1/\alpha} \tag{5}$$

For $\omega \ll \omega_{max}$ and $\omega \gg \omega_{max}$ the HN function for $M''(\omega)$ reduces to power laws with the exponents α and $\alpha\gamma$, respectively. To fit the α-process, all parameters were free, while for the β-processes

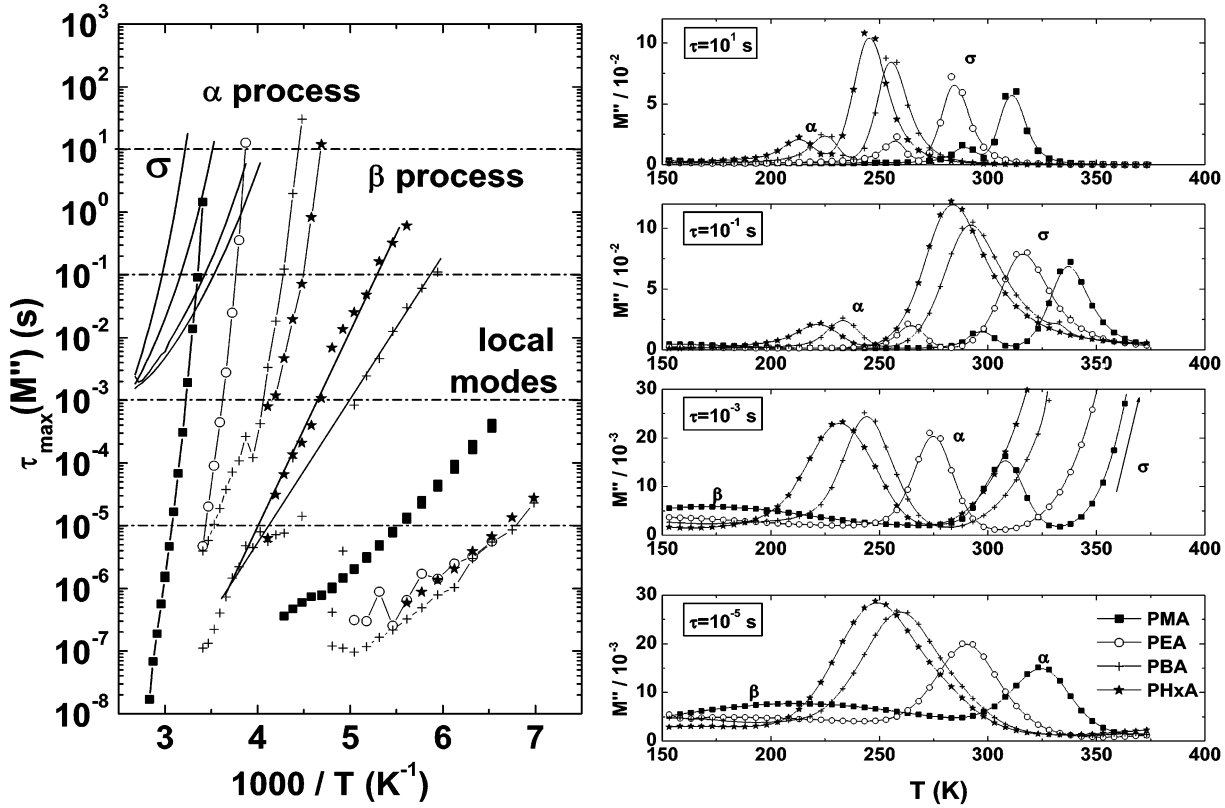

Figure 2. Temperature and frequency dependencies of the imaginary part of the dielectric modulus for the four polyacrylate samples. The Arrhenius plot yielded by fitting of the measured frequency-dependent data with frequency-dependent Havriliak−Negami functions is shown on the left. Isochronous slices through the full three-dimensional measured data set are shown on the right. The dashed−dotted lines on the Arrhenius plot on the left correspond to the correlation times of these isochronous slices. The solid lines on the right correspond to the slice through the envelope of the full three-dimensional data set (and not to a fitted function).

the asymmetry parameter γ was set to 1 (this corresponds to a symmetric peak which is typical for the β-process). Note that the HN function is usually used to fit the dielectric function and not for the dielectric modulus. However, the imaginary part of the HN function is also a good choice to describe the imaginary part of the dielectric modulus. For the real part of the modulus, of course, the HN function does not work.

Dynamic Mechanical Measurements. Dynamic mechanical measurements were performed using the ARES mechanical spectrometer (Rheometric Scientific). Shear deformation was applied under condition of controlled deformation amplitude, always remaining in the range of the linear viscoelastic response of studied samples. Geometry of parallel plates was used with plate diameters of 6 mm. The gap between plates (sample thickness) was about 1 mm. Experiments were performed under a dry nitrogen atmosphere. Frequency dependencies of G' and G'' measured within the frequency range 0.1−100 rad s^{-1} at various temperatures were used to construct master curves representing a broad range frequency dependencies of these quantities. Only shifts along the frequency scale were performed. This procedure provided a temperature dependence of shift factors (log a_T vs T). The relaxation times corresponding to the transition to the Newtonian flow range at low frequencies (τ_N) and to the glassy range at high frequencies (τ_s) at the reference temperature have been determined as $\tau(T_{ref}) = 1/\varpi$, where ϖ is the frequency at which the G' and G'' dependencies cross each other at corresponding frequency ranges. Relaxation times at another temperatures are given by log $\tau(T)$ = log $\tau(T_{ref})$ + log a_T.

Solid-State NMR. Solid-state NMR measurements were carried out on a Bruker DSX spectrometer at Larmor frequencies of 300.13 MHz for ^{1}H and 75.47 MHz for ^{13}C using commercial 7.5 mm static and 4 mm magic angle spinning (MAS) double-resonance probes from Bruker BioSpin GmbH. For the measurements done under static conditions, the actual sample temperature was calibrated using lead nitrate and a few melting points.[11]

2D-WISE spectra[15] were recorded under static conditions for PMA, PEA, PBA, and PHxA at T_g + 70 K using a 7 mm rotor. A 5 μs 90° ^{1}H pulse was used, followed by a 180° pulse in the middle of indirect time to refocus the chemical shifts, in order to acquire the static ^{1}H line width in the indirect dimension. To avoid ^{1}H spin diffusion, polarization transfer from ^{1}H to ^{13}C was accomplished by Lee−Goldburg cross-polarization,[16] with 500 μs contact time. During ^{13}C acquisition, ^{1}H continuous wave decoupling at 50 kHz rf nutation frequency was applied. 144−176 increments were acquired in the indirect ^{1}H dimension, and 240−304 transients were recorded in the direct ^{13}C dimension with 2 s relaxation delay between consecutive transients.

Lee−Goldburg cross-polarization (CP) MAS spectra were recorded at 3 kHz MAS spinning frequency using 4 mm rotors. In the ^{1}H channel the rf power level was set to a nutation frequency of 83 kHz (corresponding to a 90° pulse length of 3 μs) for excitation as well as for ^{1}H continuous wave decoupling during acquisition. A relaxation delay of 3 s was chosen for these experiments. The Lee−Goldburg irradiation[16] for the CP was adjusted on the ^{1}H nuclei by first calculating the corresponding irradiation offset frequency for the chosen rf power level and then finely adjusting the irradiation power by optimizing the resolution of ^{13}C multiplets under Lee−Goldburg decoupling conditions. The following series of experiments were conducted: first a simple LG-CP spectrum, second a LG-CP spectrum recorded immediately after a dipolar filter, and third a LG-CP spectrum recorded after a dipolar filter with the same experimental settings and a subsequent mixing time. The experiments were conducted on PEA at ca. 329 K (ca. T_g + 70 K) with a CP contact time of 1.5 ms, a filter with 20 μs delay and 4 cycles, a mixing time of 20 ms, and 2560, 5120, and 8192 transients for the three spectra, respectively. The experiments were conducted on PBA at room temperature (ca. T_g + 70 K) with a CP contact time of 3 ms, a filter with 20 μs delay and 8 cycles, a mixing time of 50 ms, and 3072, 8192, and 8192 transients for the three spectra, respectively.

The principle of the nuclear Overhauser effect (NOE) experiment with dipolar filter was presented in detail previously.[3] 62.5 kHz rf nutation frequency and 5 s recycle delay have been used. The delay between pulses in the dipolar filter has been varied from 10 to 20 μs, and the number n of cycles in the dipolar filter from 1 to 12, depending on the sample and the temperature. For each sample at each temperature, an average of the correlation times obtained with different filter parameters has been calculated. The measurements have been carried out at temperatures ranging from T_g + 75 K to T_g + 100 K on sample PMA and from T_g + 20 K to T_g + 100 K on samples PEA, PBA, and PHxA.

Results

Dielectric Spectroscopy. The dielectric measurements were done and processed as frequency-dependent measurements (see Experimental Section). Three-dimensional plots of the full data sets are given in the Supporting Information. Figure 2 (right) shows slices of these three-dimensional plots at four frequencies (10^{-1}, 10^1, 10^3, and 10^5 Hz), which are examples of the temperature dependence of the imaginary part of the dielectric modulus for the different polyacrylate samples. The corresponding relaxation processes are compiled in Figure 2 (left). At a given frequency, the α-process occurs at lower temperature with increasing side-chain length, as expected from the decreasing glass transition temperatures. Similar results were observed in the homologous series of the poly(*n*-alkyl methacrylates).[17] The β-process is only observed in the butyl and hexyl members. In the methyl and ethyl members, the intensity seems too small to detect this process (note that in a commercial poly(methyl acrylate) two local relaxations were previously observed[18]). For the butyl and hexyl members, the β-process shifts to lower frequencies with increasing side-chain length.

Furthermore, at very low temperatures and high frequencies, a further relaxation process is observed, named local mode. This process is almost independent of the side-chain length. Finally, the σ-process detected for all samples represents the conductivity of the samples. It is not a relaxation process of the polymer chains, and thus it is not of interest for the present study. The conductivity of the sample increases with increasing side-chain length.

Dynamic Mechanical Measurements. The mechanical analysis of polymers was performed in a way typically used for amorphous polymers. The properties of all samples are characterized by the frequency dependencies of the real (G') and imaginary (G'') parts of the complex shear modulus determined in a dynamic deformation experiments with sinusoidal deformation signal. The reported dependencies are master curves obtained by only frequency shifts of the spectra recorded at various temperatures to a single reference temperature (20 °C common for all samples). Figure 3 (top) shows a comparison of the master curves for various polymers. All the dependencies indicate two characteristic relaxation processes present in each polymer corresponding to a faster segmental motion and to slower chain motion detected at high and low frequencies, respectively. Most of the polymers are entangled, and the behavior observed is typical for such systems. The results indicate three different ranges of properties: glassy, rubbery, and liquidlike which are separated by the two relaxation transitions.

The relaxation times vs reciprocal temperature are shown in Figure 3 (bottom). The horizontal dashed line indicates the level of 100 s, which is often assumed as the relaxation time that the segmental motion can reach at the glass transition temperature. The DSC glass transition temperatures are indicated in Figure 3 (bottom) by means of the vertical solid lines.

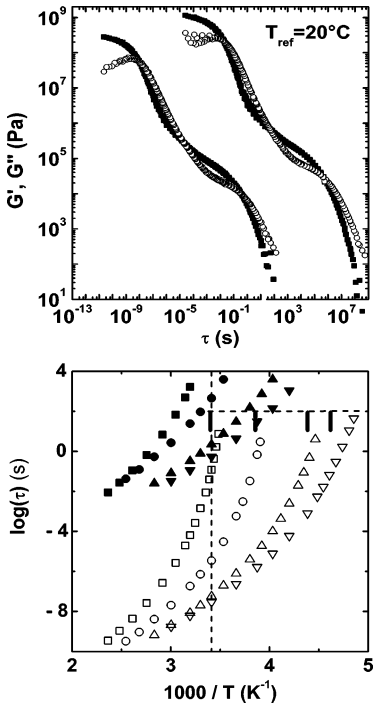

Figure 3. (top) Time dependencies (master curves at the reference temperature of 20 °C) of the real (G', solid squares) and imaginary (G'', hollow circles) components of the complex shear modulus for the studied polymers determined by dynamic mechanical measurements. From right to left: PMA, PEA, PBA, PHxA. (bottom) Relaxation times vs reciprocal temperature (activation plot) for the investigated polymers: PMA (■), PEA (●), PBA (▲), and PHxA (▼) determined by dynamic mechanical measurements. Open and filled symbols correspond to segmental and chain relaxation times, respectively. The horizontal dashed line shows the level of $\tau = 100$ s. The vertical dashed line indicates the room temperature (25 °C), and the thick vertical lines indicate glass transition temperatures determined from the DSC data (see Table 1); from left to right: PMA, PEA, PBA, and PHxA.

Solid-State NMR. The NOE experiment with dipolar filter[3] used in the present work to quantify chain dynamics in poly(*n*-alkyl acrylates) consists of a dipolar filter, selecting the magnetization in the more mobile parts of the sample, followed by a mixing time during which magnetization is transferred in the sample by a cross-relaxation (or NOE) mechanism (see Supporting Information for pulse scheme). Because of the poor resolution of ^{1}H static spectra of polyacrylates at the temperatures investigated here, the observed ^{1}H spectra exhibit an apparent single line at almost all temperatures (above $T_g + 90$ K other signals start to be distinguishable). The spectrum recorded at the end of the dipolar filter exhibits an apparent single line, which is narrower than the apparent single line observed without dipolar filter. Then for increasing mixing times τ_m, the apparent single line becomes broader, until it reaches the line width observed without dipolar filter. Several aspects need to be checked prior to quantification of chain dynamics using this experiment:[3] Is there a dynamic contrast inside the sample? What selection does the dipolar filter actually do? Is the mechanism for magnetization transfer during the mixing time actually cross-relaxation?

The dynamic contrast (difference in mobility between the more mobile and the less mobile parts of a sample) was characterized in all samples by solid-state NMR.[19] ^{1}H static spectra exhibit a line which gets narrower in a visually homogeneous way with increasing temperature.[11] This means that the whole sample is becoming more mobile with increasing temperature and exhibits no strong dynamic contrast. In order to characterize more precisely the dynamic contrast, the 2D-WISE technique[15] was used. In a 2D-WISE spectrum, the different chemical groups of the molecule are resolved according to their ^{13}C chemical shifts in the ^{13}C dimension; furthermore, the line width in the ^{1}H dimension gives a rough indication of the mobility of the corresponding group: the narrower the line, the more mobile the chemical group. 2D-WISE measurements were done at $T_g + 70$ K for all samples (see Supporting Information). In PMA, PEA, and PBA the side-chain end is significantly more mobile than the main chain, while in PHxA a mobility gradient is observed along the alkyl side chain, starting from the more mobile CH_3 end group.[11]

The selection done by the dipolar filter in the NOE experiment was checked on PEA and PBA by an independent NMR measurement: the selected ^{1}H signal was transferred to ^{13}C nuclei via Lee−Goldburg cross-polarization and acquired in the ^{13}C channel under MAS to gain chemical shift resolution.[3] The obtained ^{13}C spectra are presented in the Supporting Information. They prove that the dipolar filter actually selects the end of the alkyl side chains, namely only the CH_3 end group and partly the next CH_2 group(s).[11]

The mechanism of magnetization transfer during the mixing time was investigated by monitoring the intensity of the more mobile parts of the sample as a function of the mixing time during the exchange experiment with dipolar filter, for different filters.[3] Two mechanisms are possible. A coherent magnetization transfer via residual dipolar couplings would result in a linear dependency of the intensity with the square of the mixing time.[20] A noncoherent magnetization transfer via cross-relaxation (or NOE) results in a logarithmic dependency of the intensity on the mixing time.[3] Those plots were done for all samples at all temperatures, and the representative example of PEA at 329 K is shown in Figure 4. The logarithmic plot of recorded intensity vs mixing time is linear (in agreement with an NOE mechanism) while the plot of recorded intensity vs the square of the mixing time is clearly curved (indicating a negligible contribution of coherent magnetization transfer). Therefore, it is concluded that the magnetization transfer during the mixing time occurs predominantly via a noncoherent mechanism (although a very small contribution of coherent magnetization transfer cannot be excluded). Thus, the recorded data were treated and interpreted considering a cross-relaxation formalism for all samples at all temperatures.[3]

Concerning the equation governing the magnetization transfer, the one-dimensional NOE experiment with dipolar filter conducted in the present work is equivalent to monitoring a diagonal line intensity in a 2D NOE experiment.[3] In the investigated samples, the dipolar filter selects the end of the alkyl side chains, namely only the CH_3 end group and partly the next CH_2 group(s). Therefore, the equation corresponding to homonuclear CH_3−CH_2 system in the slow-motion limit[3] was derived from general equations given by Macura and Ernst:[21]

$$I(\tau_m) = K[3 + 2\exp(-5q\tau_C\tau_m)] \quad (6)$$

where $I(\tau_m)$ is the monitored line intensity, K a constant, q the coupling strength, τ_C the correlation time molecular motion giving rise to the cross-relaxation, and the τ_m the mixing time. The q parameter was independently measured through the second moment of the ^{1}H line recorded below T_g under static conditions:[3] 8.42 kHz^2 for PMA, 11.5 kHz^2 for PEA, 9.81 kHz^2 for PBA, and 8.77 kHz^2 for PHxA (data not shown[11]). It should be emphasized that a CH_3−CH_2 system does not strictly represent the whole monomeric unit; however, to our knowledge, no analytical equation is available for moieties larger than two groups of equivalent nuclei.

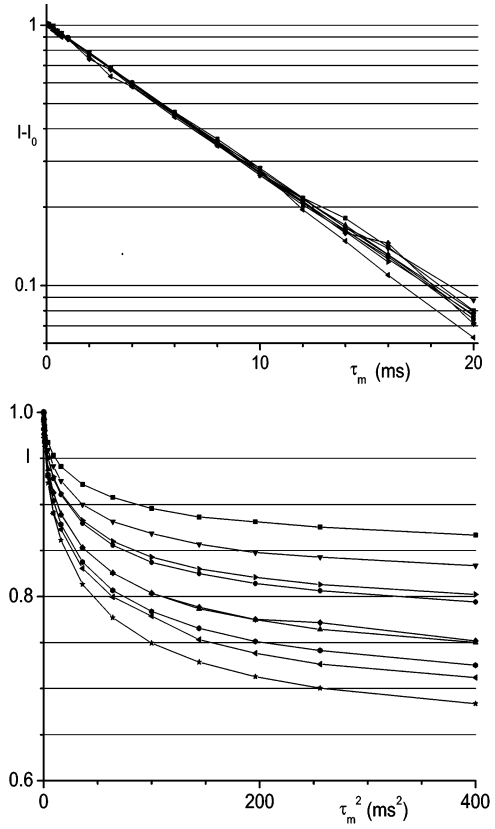

Figure 4. Evolution of the ^{1}H magnetization of mobile species for the sample PEA at 329 K with the mixing time: with the mixing time on a logarithmic scale (top); with the square of the mixing time on a linear scale (bottom). Each curve corresponds to a different set of parameters for the filter (delay between pulses, number of cycles).

The correlation times τ_C measured by NOE are plotted together with the ones of dielectric and mechanical relaxation for all samples (Figure 5). The relaxation process observed by the NMR experiment is detected on a time scale slower than the $\alpha\beta$-relaxation (cooperative α-relaxation) and at temperatures higher than the main-chain simple α-relaxation detected by dielectric spectroscopy as well as dynamic mechanical measurements at the same temperature (both exhibiting similar traces, Figure 5). Individual larger scale Arrhenius plots for each sample and numerical values are given in the Supporting Information.

Discussion

The relaxation process observed with the NMR experiment is detected on a time scale slower than the $\alpha\beta$-relaxation (cooperative α-relaxation) and at temperatures higher than the main-chain simple α-relaxation detected by dielectric spectroscopy and dynamic mechanical measurements (both exhibiting similar traces, Figure 5). This relaxation process in poly(*n*-alkyl acrylates) is detected and quantified for the first time on such a time scale and temperature range. It should be underlined here that different relaxation processes may be detected by NOE with dipolar filter and by dielectric spectroscopy due to different detection methods. The dielectrics indeed primarily detects motions via the permanent dipole located at the carbonyl group in the laboratory frame, while the NOE probes motions more locally via relative motions of neighboring ^{1}H nuclei causing a modulation of the dipolar coupling in their local molecular frame. The NOE experiment actually detects the motion of the group selected by the dipolar filter (predominantly the CH_3 group) together with the group(s) to which it is transferring magnetization (the next CH_2 group(s)), as a whole, with respect to their environment.

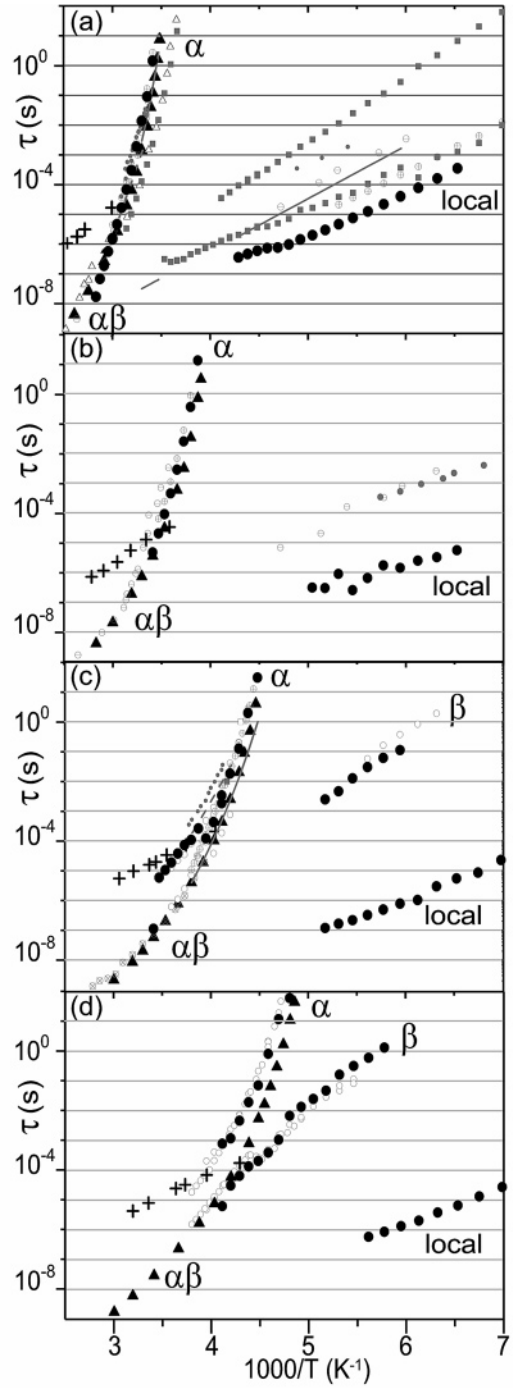

Figure 5. Arrhenius plot of the correlation times extracted for samples PMA (a), PEA (b), PBA (c), and PHxA (d) using solid-state NMR (+), dielectric spectroscopy (●), and mechanical spectroscopy (▲). The experimentally measured values (black symbols) are plotted together with literature values (grey symbols) from dielectric relaxation spectroscopy: Beiner et al.[8] (○), Buerger et al.[27] (—, PMA), de Brouckere et al.[28] (– –), Fioretto et al.[29] (⊗), Fitzgerald et al.[30] (—, PBA), Gomez-Ribelles et al.[31,32] (●), Hayakawa et al.[33] (■, – –, PBA), Jourdan et al.[34] (□), Kahle[35] (■, PMA), Mead et al.[36] (⊖), McCrum[25] (⊖), Reissig[37] (⊕); and from mechanical spectroscopy: Gomez-Ribelles et al.[32] (▲) and Soen et al.[38] (△). Larger plots for individual samples are available in the Supporting Information.

The poly(*n*-alkyl acrylates) investigated here exhibit a local nanostructure, as shown by WAXS results (see Supporting Information). The geometry of this local structure is not known

precisely, except that it involves nanodomains of side chains.[8] Previously investigated poly(*n*-alkyl methacrylates) are similar in chemical nature and exhibit a layered structure, in which disordered sheets of aligned main chains are separated by layers of side chains.[22] By analogy with poly(*n*-alkyl methacrylates), the relaxation process observed by NMR in poly(*n*-alkyl acrylates) could be the isotropization of the main chain, which was recently detected for poly(*n*-alkyl methacrylates) on a time scale slower than the conventional α-relaxation.[17,23] This isotropization process arises because the polymer melt is locally structured and because of the presence of extended backbone conformations; thus, the isotropization of the backbone conformation needs many steps of restricted locally axial chain motion.[17,23] The NMR relaxation data together with the dielectric simple α-relaxation data were fitted for all samples to a WLF equation:[24]

$$\log\left(\frac{\tau_C}{\tau_{Cg}}\right) = \frac{-C_1(T - T_g)}{C_2 + T - T_g} \tag{7}$$

where τ_{Cg} is 100 s, T_g is the glass transition temperature, and C_1 and C_2 are the WLF coefficients. Physically sound values were found for the fitted processes: $C_1 = 9$ and $C_2 = 17$ K for PMA, $C_1 = 9$ and $C_2 = 15$ K for PEA, $C_1 = 8$ and $C_2 = 13$ K for PBA, $C_1 = 8$ and $C_2 = 20$ K for PHxA (see Supporting Information for more details). Furthermore, the respective T_g values found by WLF fits (289, 257, 225, and 211 K) are in agreement with those measured by DSC (Table 1). Thus, the relaxation process observed by NMR could be the isotropization of the main chain in poly(*n*-alkyl acrylates). However, the main-chain isotropization relies on the main-chain rigidity for polymethacrylates, yet polyacrylates have a significantly more flexible main chain. Thus, the isotropization process for polyacrylates is expected to take place on a significantly faster time scale than for polymethacrylates. Moreover, for PBA and PHxA the correlation times measured by NMR at the lowest temperature ($T_g + 20$ K) seem to fall outside of the common trace of dielectric spectroscopy and NMR fitted by the WLF equation, and at the crossover between the dielectric and NMR data, the apparent activation energies of the processes detected by each method are different. Furthermore, it might seem surprising that the relaxation process detected by NMR is slower but has a lower apparent activation energy than the α-relaxation process detected by dielectric and mechanical spectroscopy, but this is also observed for the isotropization and α-relaxation processes in poly(*n*-alkyl methacrylates).[17,23] Finally, the interpretation of the relaxation process detected by NMR in terms of main-chain motion is questionable due to the selection done by the dipolar filter at the beginning of the NMR experiment: only the end of the local side chain is selected. Therefore, the NMR technique is expected to detect a relaxation of the side chain, which seems to be in contradiction with the possible detection of the isotropization of the main chain.

Assuming that the NMR experiment would detect a local relaxation process within the side chain, it is consistent to assume an Arrhenius behavior for it. The resulting linear dependence of the correlation time τ_C on inverse temperature is in agreement with the experimental data, although those data were acquired on a too narrow temperature range to allow any conclusion on a possible curvature. The experimental data were fitted to the Arrhenius equation for all samples:

$$\tau_C = A \exp\left(\frac{E_a}{RT}\right) \tag{8}$$

where A is the preexponential factor, E_a is the activation energy of the relaxation process, R is the gas constant, and T is the absolute temperature. The values found for preexponential factor and apparent activation energy were 2×10^{-13} s and 22 kJ mol^{-1} for PMA, 6×10^{-13} s and 18 kJ mol^{-1} for PEA, 6×10^{-11} s and 13 kJ mol^{-1} for PBA, and 9×10^{-11} s and 12 kJ mol^{-1} for PHxA, respectively. More details on linear regression of correlation and relaxation times for the process detected by NOE as well as the *β*-relaxation process and the relaxation process labeled as "local" can be found in the Supporting Information. For PBA and PHxA, the activation energy of the process detected by NOE is intermediate between those of the local relaxation and of the *β*-relaxation (10 and 18 kJ mol^{-1}, respectively, for PBA; 10 and 15−25 kJ mol^{-1} for PHxA). For PEA and PMA, the activation energies of the process detected by NOE are also higher than those of the local relaxation (ranging respectively from 8 to 14 kJ mol^{-1} and from 11 to 19 kJ mol^{-1}). Please note that for PMA and PEA no *β*-relaxation process was detected by dielectric spectroscopy. However, it could be present but insufficiently resolved from the simple α-relaxation process due to proximity in frequency and a lower intensity of the *β*-relaxation (it might be detectable by mechanical measurements with another geometry). The simple α-relaxation is usually attributed to motions of the main chains, α*β*-relaxation (cooperative α-relaxation) to motions of the main chains coupled to reorientations of the side chains, *β*-relaxation to reorientations of the whole COO−alkyl side chains, and local

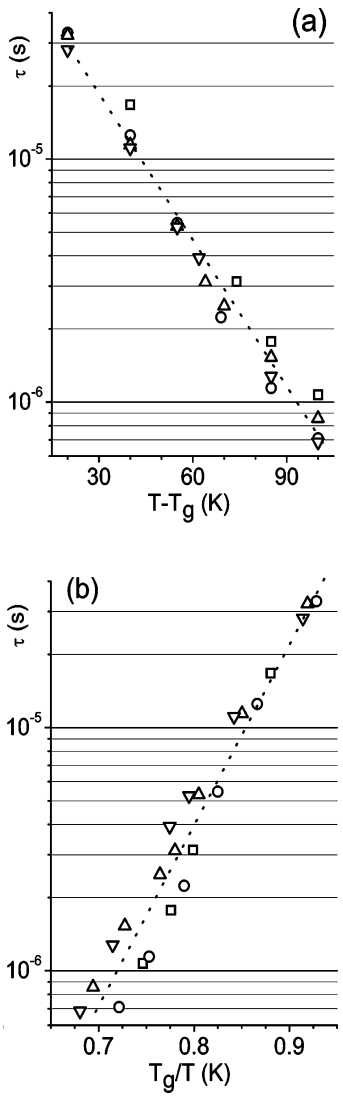

Figure 6. Correlation times extracted for samples PMA (□), PEA (○), PBA (Δ), and PHxA (▽) using solid-state NMR, plotted vs (a) the temperature difference to the glass transition temperature and (b) the inverse temperature multiplied by the glass transition temperature.

relaxation to reorientations of parts of these side chains in poly(alkyl acrylates).[25] Thus, the process detected by NOE could logically be assigned to reorientations of parts of the side chains, i.e., to a superposition of β-relaxation and more local relaxation. The relaxation process detected by NMR would then be the continuation at high temperature of a local relaxation process usually observed at temperatures lower than that of the α-relaxation. This would be in agreement with a lower activation energy than that of the α-relaxation. Nevertheless, it might seem surprising that the corresponding motions of the side chain be slower than those of the main chain (α- and $\alpha\beta$-relaxations) in the temperature range where the measurements were carried out. However, in the context of locally organized samples investigated by different methods, it is conceivable that some side-chain motions would be slower than those of the main chain. Observation of a relaxation process does not imply that such a process leads to complete relaxation of main chains and side chains.[17,23] This leaves room for detecting additional relaxation via another technique on longer time scales. Thus, time scale and amplitude of relaxation processes should clearly be distinguished (see, e.g., ref 26). Indeed, the α- and $\alpha\beta$-relaxation processes of the main chains are detected by dielectric (and mechanical) spectroscopy, while the new relaxation process is detected by NOE NMR. Dielectric spectroscopy primarily detects motion in the laboratory frame via the permanent dipole located at the carbonyl group. The NOE experiment probes motions more locally via relative motions of neighboring ^{1}H nuclei, causing a modulation of the dipolar coupling in their local molecular frame. Therefore, the α-relaxation and the relaxation process probed by NOE are detected in different frames (respectively local molecular frame and laboratory frame). Furthermore, as detailed above, the poly(*n*-alkyl acrylates) investigated here exhibit a local nanostructure, which involves nanodomains of side chains. The existence of the local nanodomains restricts the motion of the involved side chains with respect to their neighbors. Thus, the side chains might reorient within the nanodomain in the local molecular frame on a time scale longer than that of the main-chain α- and $\alpha\beta$-relaxation in the laboratory frame. The NOE experiment would then detect hindered motions of the side chains inside the nanodomains in the local molecular frame, resulting from β-relaxation and more local relaxations.

Finally, an interesting property was observed for the relaxation process measured by NMR. Although the measured correlation times depend on the alkyl side-chain length, they become sample-independent when plotted as a function of the temperature difference to T_g or of the inverse temperature by T_g (Figure 6).

Conclusions

Through NMR measurements with a recently developed solid-state NMR method (NOE with dipolar filter), a relaxation process was detected in various members of the poly(*n*-alkyl acrylates) family, in the melt. This relaxation process occurs at a higher temperature than does the simple α-relaxation and on a longer time scale than that of the $\alpha\beta$-relaxation (cooperative α-relaxation). It was detected and quantified for the first time on these temperature and time scales.

Because of the presence of branching in polyacrylates, dielectric spectroscopy and dynamic mechanical measurements were conducted on the same samples to help interpreting the NMR results. The relaxation process detected in polyacrylates could be the isotropization of the main chain, by analogy with structurally similar poly(*n*-alkyl methacrylates). It is more probably a local relaxation within the alkyl side chain that is usually detected only at significantly lower temperatures. The fact that this side-chain motion is slower than the cooperative main-chain α-relaxation is striking but can be rationalized in the context of locally nanostructured samples investigated by methods detecting motion in different frames. A definitive molecular assignment of the relaxation process detected by the NOE NMR method requires further investigation. It could be done by advanced solid-state NMR techniques with selectively ^{2}H- or ^{13}C-labeled samples.

Acknowledgment. M.G. thanks Arkema and Total for financial support. Dr. Patrice Castignolles is thanked for multidimensional SEC measurements and Andreas Hannewald for measurements of mechanical spectroscopy.

Supporting Information Available: Details of experimental conditions, complementary X-ray scattering and NMR results, numerical values for relaxations processes and larger Arrhenius plots. This material is available free of charge via the Internet at http://pubs.acs.org.

References and Notes

(1) Penzel, E. Polyacrylates. In *Ullmann's Encyclopedia of Industrial Chemistry*, 7th ed.; Wiley-VCH: Weinheim, Germany, 2005; Vol. A21.
(2) Sprong, E.; Leswin, J. S. K.; Lamb, D. J.; Ferguson, C. J.; Hawkett, B. S.; Pham, B. T. T.; Nguyen, D.; Such, C. H.; Serelis, G. K.; Gilbert, R. G. *Macromol. Symp.* **2006**, *231*, 84−93.
(3) Gaborieau, M.; Graf, R.; Spiess, H. W. *Solid State Nucl. Magn. Reson.* **2005**, *28*, 160−172.
(4) Ahmad, N. M.; Heatley, F.; Lovell, P. A. *Macromolecules* **1998**, *31*, 2822−2827.
(5) Farcet, C.; Belleney, J.; Charleux, B.; Pirri, R. *Macromolecules* **2002**, *35*, 4912−4918.
(6) Asua, J. M.; Beuermann, S.; Buback, M.; Castignolles, P.; Charleux, B.; Gilbert, R. G.; Hutchinson, R. A.; Leiza, J. R.; Nikitin, A. N.; Vairon, J. P.; van Herk, A. M. *Macromol. Chem. Phys.* **2004**, *205*, 2151−2160.
(7) Miller, R. L.; Boyer, R. F.; Heijboer, J. *J. Polym. Sci., Part B: Polym. Phys.* **1984**, *22*, 2021−2041.
(8) Beiner, M.; Huth, H. *Nat. Mater.* **2003**, *2*, 595−599.
(9) Stadler, F. J.; Piel, C.; Klimke, K.; Kaschta, J.; Parkinson, M.; Wilhelm, M.; Kaminsky, W.; Munstedt, H. *Macromolecules* **2006**, *39*, 1474−1482.
(10) Wood-Adams, P. M.; Dealy, J. M.; deGroot, A. W.; Redwine, O. D. *Macromolecules* **2000**, *33*, 7489−7499.
(11) Gaborieau, M. Solid-state NMR investigation of spatial and dynamic heterogeneity in acrylic pressure sensitive adhesives (PSAs) compared to model poly(n-alkyl acrylates) and poly(n-alkyl methacrylates) Ph.D. Thesis, University Louis Pasteur, Strasbourg, France, 2005.
(12) Gaborieau, M.; Gilbert, R. G.; Gray-Weale, A.; Hernandez, J. M.; Castignolles, P. *Macromol. Theory Simul.* **2007**, *16*, 13−28.
(13) Havriliak, S.; Negami, S. *Polymer* **1967**, *8*, 161−210.
(14) Kahle, S.; Schroter, K.; Hempel, E.; Donth, E. *J. Chem. Phys.* **1999**, *111*, 6462−6470.
(15) Schmidt-Rohr, K.; Clauss, J.; Spiess, H. W. *Macromolecules* **1992**, *25*, 3273−3277.
(16) Lee, M.; Goldburg, W. I. *Phys. Rev.* **1965**, *140*, A1261−A1271.
(17) Wind, M.; Graf, R.; Renker, S.; Spiess, H. W. *Macromol. Chem. Phys.* **2005**, *206*, 142−156.
(18) Kahle, S., unpublished results.
(19) Schmidt-Rohr, K.; Spiess, H. W. *Multidimensional Solid-State NMR and Polymers*, 1st ed.; Academic Press: San Diego, CA, 1994.
(20) Demco, D. E.; Hafner, S.; Fulber, C.; Graf, R.; Spiess, H. W. *J. Chem. Phys.* **1996**, *105*, 11285−11296.
(21) Macura, S.; Ernst, R. R. *Mol. Phys.* **2002**, *100*, 135−147.
(22) Wind, M.; Graf, R.; Renker, S.; Spiess, H. W.; Steffen, W. *J. Chem. Phys.* **2005**, *122*, 0149061−01490610.
(23) Wind, M.; Graf, R.; Heuer, A.; Spiess, H. W. *Phys. Rev. Lett.* **2003**, *91*, 1557021−4.
(24) Williams, M. L.; Landel, R. F.; Ferry, J. D. *J. Am. Chem. Soc.* **1955**, *77*, 3701−3707.
(25) McCrum, N. G.; Read, B. E.; Williams, G. Methacrylates and related polymers. In *Anelastic and Dielectric Effects in Polymeric Solids*; Dover Publications: New York, 1991; pp 238−299.
(26) Hirschinger, J.; Miura, H.; Gardner, K. H.; English, A. D. *Macromolecules* **1990**, *23*, 2153−2169.
(27) Buerger, D. E.; Boyd, R. H. *Macromolecules* **1989**, *22*, 2694−2699.
(28) de Brouckere, L.; Offergeld, G. *J. Polym. Sci.* **1958**, *30*, 105−118.
(29) Fioretto, D.; Livi, A.; Rolla, P. A.; Socino, G.; Verdini, L. *J. Phys.: Condens. Matter* **1994**, *6*, 5295−5302.
(30) Fitzgerald, J. J.; Binga, T. D.; Sorriero, L. J.; Oreilly, J. M. *Macromolecules* **1995**, *28*, 7401−7406.

(31) Gomez Ribelles, J. L.; Meseguer Duenas, J. M.; Monleon Pradas, M. *J. Appl. Polym. Sci.* **1989**, *38*, 1145−1157.
(32) Gomez Ribelles, J. L.; Monleon Pradas, M.; Mas Estelles, J.; Meseguer Duenas, J. M.; Romero Colomer, F. *Plast. Rubber Compos. Process. Appl.* **1992**, *18*, 169−179.
(33) Hayakawa, T.; Adachi, K. *Polym. J.* **2000**, *32*, 845−848.
(34) Jourdan, C.; Cavaille, J. Y.; Perez, J. *Polym. Eng. Sci.* **1988**, *28*, 1318−1325.
(35) Kahle, S., personal communication, Mainz, Germany, 2004, alpha- and beta-relaxation in poly(methyl acrylate).
(36) Mead, D. J.; Fuoss, R. M. *J. Am. Chem. Soc.* **1942**, *64*, 2389−2393.
(37) Reissig, S. Dielektrische und kalorimetrische Untersuchungen des Einflusses molekularer Details auf das $\alpha\beta$-Splittingsverhalten der Poly-(n-alkylmethacrylate). Ph.D. Thesis, Martin Luther University, Halle, Germany, 1999.
(38) Soen, T.; Yamashit, K.; Kawai, H.; Ono, T. *Kolloid Z. Z. Polym.* **1972**, *250*, 459−470.

MA0706531